



HAL
open science

Potentialities of a mesoporous activated carbon as virus detection probe in aquatic systems

Doriane Delafosse, Laurence Reinert, Philippe Azaïs, Dominique Fontvieille,
Yasushi Soneda, Patrice Morand, Laurent Duclaux

► To cite this version:

Doriane Delafosse, Laurence Reinert, Philippe Azaïs, Dominique Fontvieille, Yasushi Soneda, et al.. Potentialities of a mesoporous activated carbon as virus detection probe in aquatic systems. *Journal of Virological Methods*, 2022, 303, pp.114496. 10.1016/j.jviromet.2022.114496 . hal-03591925

HAL Id: hal-03591925

<https://univ-smb.hal.science/hal-03591925v1>

Submitted on 22 Jul 2024

HAL is a multi-disciplinary open access archive for the deposit and dissemination of scientific research documents, whether they are published or not. The documents may come from teaching and research institutions in France or abroad, or from public or private research centers.

L'archive ouverte pluridisciplinaire **HAL**, est destinée au dépôt et à la diffusion de documents scientifiques de niveau recherche, publiés ou non, émanant des établissements d'enseignement et de recherche français ou étrangers, des laboratoires publics ou privés.



Distributed under a Creative Commons Attribution - NonCommercial 4.0 International License

1 **Title: Potentialities of a mesoporous activated carbon as virus detection probe in aquatic**
2 **systems**

3
4 **Authors:** Doriane Delafosse^{a,b,*}, Laurence Reinert^c, Philippe Azaïs^d, Dominique Fontvieille^a, Yasushi
5 Soneda^e, Patrice Morand^b, Laurent Duclaux^c

6
7 **Affiliations:**

8 ^a Laboratoire Abiolab-Asposan, Montbonnot-Saint-Martin, France

9 ^b Université Grenoble Alpes, CNRS, CEA, Institut de biologie structurale (IBS), Grenoble, France

10 ^c Université Savoie Mont Blanc, EDYTEM, F-73000 Chambéry, France

11 ^dCEA-LITEN, DEHT, Grenoble, France

12 ^e National Institute of Advanced Industrial Science and Technology (AIST), Energy Process Research
13 Institute, Tsukuba, Ibaraki 305-8569, Japon

14 * Corresponding author. E-mail address: doriane.delafosse@abiolab.fr (D. Delafosse)

15

16 **Abstract**

17 Enteric viruses are widely spread in water environments, some being harmful for human communities.
18 Regular epidemics highlight the usefulness of analysing such viruses in wastewaters as a tool for
19 epidemiologists to monitor the extent of their dissemination among populations. In this context,
20 CNovel™ Powdered Activated Carbon (PAC) was chosen for its high porosity and high adsorption
21 capacity to investigate sorbent ability to be used as part of virus detection probes. Self-supported
22 PAC Foils (PAC-F), PAC coated Brushes (PAC-B) and PAC Sampler (PAC-S) were used to prospect
23 PAC efficacy in virus adsorption and above all, the feasibility of virus retrieval from them, allowing to
24 further analysis such as molecular analysis quantification. Aiming at the development of a field-
25 operational tool, PAC saturation and reusability were also investigated, as well as PAC-polarisation
26 effect on its adsorption capacity.

27 Our results pointed out that sorbent-based probes exhibited a high adsorption efficacy of spiked
28 Murine Norovirus (MNV-1) in bare 0.1 M NaCl solution (>90% for PAC-B and >86% for PAC-F at $\approx 10^7$
29 genome unit virus concentration), with no saturation within our experimental framework. On the other
30 hand, polarisation assays using PAC-F as electrode, did not demonstrate any adsorption

31 improvement. Experiments on PAC probes reusability suggested that they should be used three times
32 at the most for a maximum efficiency. Values of virus retrieval were low (up to 11% with PAC-B and up
33 to 14% with PAC-F in 0.1M NaCl virus suspensions), illustrating the need for the techniques to be
34 improved. A preliminary field assay using PAC-S, demonstrated that our catch-and-retrieve protocol
35 yielded to the detection of autochthonous human Norovirus Genogroup I (NoV GI) and Adenovirus
36 (AdV), in wastewaters suggesting its promising application as virus detection tool in such high loaded
37 and complex waters.

38

39 **Keywords**

40 Enteric viruses – Powdered activated carbon – Sorbent-based probe – Virus analysis – Wastewater
41 analysis

42

43 **1. Introduction**

44 Human Enteric Viruses (HEV) are the main cause of waterborne diseases contracted all over the
45 world, such as gastroenteritis and hepatitis (Enserink *et al.*, 2015; Bouseettine *et al.*, 2020). Their
46 replication occurs within the gastrointestinal tract of their hosts, leading to large numbers of viruses
47 excreted together with the faeces, up to 10^{12} particles.g⁻¹ of faeces, then entering wastewaters (Gerba,
48 2000; Blacklow and Greenberg, 1991).

49 Sewers drive wastewaters to WasteWaters Treatment Plants (WWTPs) where they are processed to
50 eliminate most of their organic and mineral loads, targeting downstream aquatic systems protection.

51 However, HEV persistence in water environment, as well as a relative resistance to WWTPs
52 depollution processes, have been demonstrated (Bae and Schwab *et al.*, 2008; Seitz *et al.* 2011; Qiu
53 *et al.*, 2015; Kauppinen *et al.*, 2018). Residual virus loads in WWTP effluents reaching downstream
54 recreational or shellfish farming waters, are yet high enough to represent a public health issue (Aslan
55 *et al.*, 2011; Sinclair *et al.*, 2009).

56 Despite an increasing number of studies dedicated to this topic, a lack of efficient and standardised
57 techniques remains, especially in collecting viruses from complex media such as wastewaters.

58 In most previous researches, wastewater virus analysis follows an extraction / detection two-steps
59 protocol (Hmaied *et al.*, 2016; Cioffi *et al.*, 2020; Janahi *et al.*, 2020), where molecular analyses

60 remain the gold standard in virus appraisal. Today, they allow very low viral genome copies detection

61 (Sharkey *et al.*, 2021) while enduring some lingering impediments, as from inhibitors effects, despite
62 recurrent investigations seeking at their reduction (Albinana-Gimenez *et al.*, 2009; Canh *et al.*, 2019).

63 Particles' extraction remains the main problematic step in virus analysis, especially in addressing
64 highly diversified and heavy loaded sewage waters.

65 A large panel of methods are described in the literature about enteric virus recovery from wastewater.
66 Filtration with negatively or positively charged filters is among the most popular techniques (Ahmed *et al.*
67 *et al.*, 2015; Soto-Beltran *et al.*, 2013), together with protein precipitation (using polyethylene glycol, for
68 example) or flocculation with skimmed milk (Masclaux *et al.*, 2013; Hjelmso *et al.*, 2017; Strubbia *et al.*
69 *et al.*, 2019). Ultracentrifugation and ultrafiltration are also used as concentrating techniques (Sidhu *et al.*
70 *et al.*, 2018; Prado *et al.*, 2019; Prata *et al.*, 2012; Martín-Díaz *et al.*, 2018).

71 As successful contributors to pollutants removal in wastewater treatment processes, adsorbents may
72 appear as good candidates for virus sampling (Crini *et al.*, 2018). Among them, activated carbon,
73 under its many different formats, has been thoroughly studied for its ability to adsorb a wide range of
74 organic and inorganic components, including viruses (Cookson and North, 1967; Gerba *et al.*, 1975;
75 Powell *et al.*, 2000; Matsushita *et al.*, 2013; Cormier *et al.*, 2014). Activated carbon is a complex,
76 structurally disordered and highly porous material, available under several physical shapes (powder,
77 granules, beads, fabric, etc.). Its adsorption efficiency especially relates to its porosity, yet not being
78 specifically claimed to be mainly determinant in any of the above-mentioned studies. It can also be
79 polarised after addition of conducting additives (Goldin *et al.*, 2005; Robles *et al.*, 2020), a design
80 which may help collecting electric charges-bearing particles like virus within some pH ranges.

81 Our goal, in this work, was to setup devices and protocols committed to virus detection while
82 addressing the challenging task (as quoted by Cormier *et al.*, 2014) of operating PAC.

83 Virus adsorption on PAC rely upon several parameters:

- 84 1. PAC specifications, especially specific surface area, porous volume and pore size distribution
- 85 2. Geometry and composition of holding structures used to operate PAC (*i.e.* supports)
- 86 3. Chemical mixtures entering the build of the above mentionned structures (glues)
- 87 4. Coating evenness, especially in its thickness
- 88 5. Experimental conditions (exposition time, stirring, temperature, etc.)

89 6. Overall water composition: dissolved and particulate matters (mineral and organic) including
90 virus concentration.

91 7. Virus size, envelope, isoelectric point (IP).

92 Investigations on parameters 2 and 5, only are reported in this paper using the CNovel™ mesoporous
93 (50nm) PAC arranged in three forms:

94 - PAC foils (PAC-F), used as-is or, polarised as self-supported electrodes,

95 - PAC-coated brushes (PAC-B), an in-house design set to maximise PAC active surface,

96 - PAC sampler probes (PAC-S) designed to enter an automatic sampler committed to field
97 experiments.

98 All our experiments aimed at the assessment of both, PAC virus adsorption capacities and virus
99 recovery efficiency after desorption. PAC abilities to enter field operational virus sampling tools were
100 also investigated. Indeed, PAC probes, should not only be efficient in collecting viruses from aqueous
101 media, but also in allowing their release, or at least, part of it, for further genome identification and
102 quantification by Reverse Transcription-quantitative Polymerase Chain Reaction (RT-qPCR). We also
103 investigated a possible saturation of our PAC material after few adsorption steps, its ability to be
104 reused through successive virus adsorption/recovery cycles and the effect of polarisation on its
105 adsorption capacity.

106

107 **2. Materials and Methods**

108 All experiments were conducted on 0.1M NaCl Murine Norovirus suspensions and on wastewaters
109 from the WWTP of the Grand-Chambery urban community (Savoie, France).

110

111 **2.1. Virus stock production**

112 The murine norovirus (MNV-1) strain, a surrogate of human norovirus was used to perform all *in vitro*
113 experiments. They were grown on murine macrophage cell line RAW 264.7 (ATCC TIB-71). High-
114 glucose Dulbecco's Modified Eagle Medium (DMEM) and Foetal Bovine Serum (FBS) were purchased
115 respectively from Corning (Corning, NY, USA) and Dominic Dutscher (Bernolsheim, France).

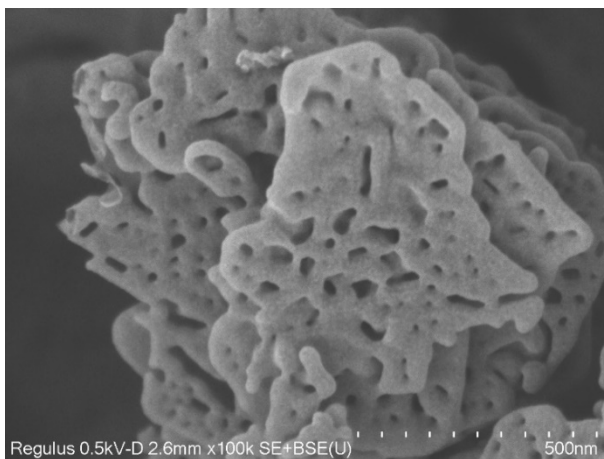
116 MNV-1 was propagated by infection of confluent RAW 264.7 cell line cultured in DMEM supplemented
117 with 5% FBS and 1% Ampicillin/Streptomycin. After 48h at 37°C under a 5% CO₂ atmosphere, lysate

118 was clarified by centrifugation at 3,000 g for 20 min at 4°C. MNV-1 containing supernatant was
119 aliquoted and stored at -80°C. Stocks were quantified by Tissue Culture Infective Dose 50% (TCID50)
120 and RT-qPCR.

121

122 **2.2. Preparation of the powdered activated carbon probes**

123 All experiments were performed with CNovel™ (Toyo Tanso Co, Osaka, Japan) mesoporous
124 activated carbon (Figure 1). Microporous and mesoporous volume are 0.209 cm³.g⁻¹ (pores diameter <
125 2 nm) and 0.855 cm³.g⁻¹ (pores diameter 2-50 nm) respectively. The BET specific surface area is 660
126 ± 3 m².g⁻¹ (P/P^o range = 0.01-0.05). As Noroviruses are around 30 nm in diameter, carbon porosity
127 centred to 50 nm in diameter (estimation from BJH method applied on adsorption branch), was chosen
128 to maximise the virus-adsorbent interaction.



129

130 *Figure 1. Scanning electron microscopy image of CNovel™ 50 nm.*

131 Within the investigated water solutions pH range (6.5-7.5), the CNovel™ zeta potential (+0.55 mV at
132 pH 7) should favour the adsorption of negatively charged Norovirus.

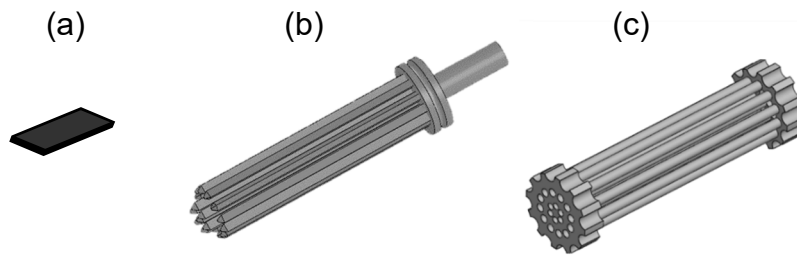
133 The three designed CNovel™-based probes are represented in Figure 2:

134 - self-supported PAC-F used as-prepared or as electrodes to investigate the role of polarity in
135 adsorption processes;

136 - PAC-B; a field operational tool candidate

137 - PAC-S, part of an automatic sampler, used in wastewater field experiments.

138



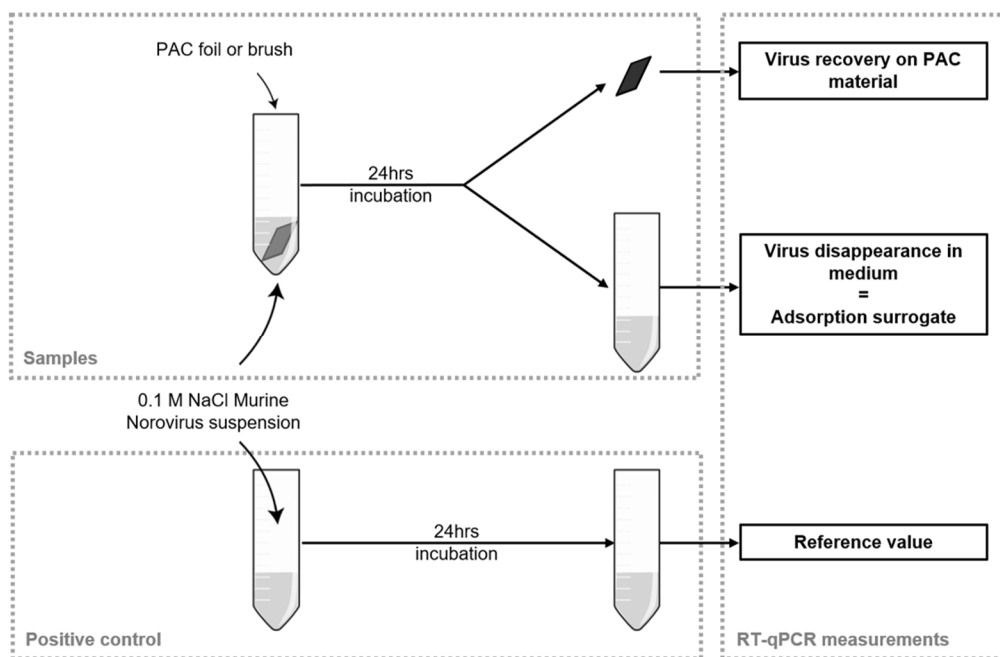
140 *Figure 2. PAC Foil (a), Brush (b) and Probe (c) designs.*

141 Brushes (PAC-B) and sampler probes (PAC-S) were 3D-printed using Polyamide 12 (nylon) or Rigid
 142 10K (resin), then coated with a mixture of 87% CNovel™ carbon, 8% PVDF Solvay 5130 and 7%
 143 conductive carbon black C65 (Imerys Graphite and Carbons). Total coated surface was about 131
 144 cm². Coating mass was = 1.2 ± 0.3 g. The coating slurry solvent was N-Methyl-2-Pyrrolidone.

145 PAC-F were prepared from 80% of porous carbon mixed with 14% of PTFE and 6% of conductive
 146 carbon black (solvent: same as above). Their total mass was = 0.038 ± 0.012 g. Foils were totally
 147 immersed (4 cm²) into the virus suspension for reusability experiments, and partly immersed (2 cm²)
 148 for polarisation assays.

149

150 2.3. Adsorption assays



151

152 *Figure 3. Adsorption assays experimental design using PAC-F (foils) or PAC-B (brushes).*

153 Both, PAC-F and PAC-B were used for these assays. All experiments were performed in triplicates at
154 room temperature (20°C) in 0.1 M NaCl MNV-1 suspension ($1.76 \cdot 10^7 \pm 0.36 \cdot 10^7$ genome units.mL⁻¹ for
155 PAC-F experiments, $2.57 \cdot 10^7 \pm 0.25 \cdot 10^7$ genome units.mL⁻¹ for PAC-B ones). They were set up to
156 emphasize virus - adsorbent contact (stirring, narrow between-foil distance).
157 PAC-F were, each, plunged into 2 mL MNV-1 suspension and incubated under a 120 rpm stirring.
158 After a 24 h contact time, the foil was transferred into another tube where virus recovery later would
159 take place (Figure 3). The NaCl solution, now freed from the foil, was submitted to RNA extraction for
160 measuring the non-adsorbed viruses' amount.
161 PAC coated brushes were, each, plunged into 30 mL MNV-1 suspension in a 50 mL test tube. Tubes
162 were incubated on a reciprocal shaker set at 120 rpm. After a 24 h contact time, PAC-B and 0.1 M
163 NaCl solution were separated and submitted to nucleic acids extraction processes.
164 In all cases, virus "disappearances" were calculated from virus concentration differences, between
165 positive controls and virus suspensions, at the end of the contact time period. Hence, these values
166 were indirect assessments of the PACs adsorption capacities.
167 Positive controls were viral suspensions at the same initial virus concentrations which had no contact
168 with an adsorbent. As such, they were used as references for recovery rate calculations. Negative
169 controls were plain 0.1 M NaCl solutions receiving a PAC device (PAC-F or PAC-B). Both controls
170 were incubated 24 h under stirring.

171
172 Investigation on a possible saturation of PAC-F adsorption capacity, by immersion of a foil into 2
173 mL virus suspension, was repeated three times (same protocol as above), using the same foil but with
174 a new virus suspension at the same initial concentration. Each time, the remaining virus concentration
175 was measured and PAC adsorption capacity calculated (Figure 3).

176

177 **2.4. Adsorption kinetics assays**

178 Assays were conducted following the previously described PAC-B adsorption protocol for , except that
179 1 mL was sampled 1 h, 2 h, 5 h, 15 h and 24 h after the experiment starting. Concentrations of the
180 remaining virus were measured and plotted over contact time.

181

182 **2.5. Experiments on PAC probes reusability**

183 Virus desorption from the probes (foils or brushes) and remaining virus in the 0.1 M NaCl suspension
184 were both investigated.

185 Experiments were performed according to the above-mentioned PAC-F and PAC-B adsorption
186 protocol, and repeated three times.

187

188 **2.6. PAC-F polarization assays**

189 Three experiments were performed with PAC-F used as electrodes: anode first, then as cathode and
190 lastly with no polarity. In each case, the counter electrode was a platinum foil, as neutral, non-
191 adsorbent material.

192 Electrodes were plunged in a 0.1 M NaCl MNV-1 suspension for 24 h at room temperature and
193 120 rpm stirring. They were connected to a DC generator set to 0.9 V. Electrodes and suspension
194 were then separated and submitted to nucleic acids extraction processes.

195

196 **2.7. Wastewater virus sampling using adsorbent based probes**

197 Field scale studies, operating an in-house built automat, were performed at the Grand-Chambéry
198 WWTP (Chambéry, France), aiming to sample autochthonous NoV GI and AdV. The plant is
199 processing both, industrial and domestic wastewaters from approximately 260,000 people over a usual
200 two steps, physicochemical, primary and biofiltration, secondary, treatment.

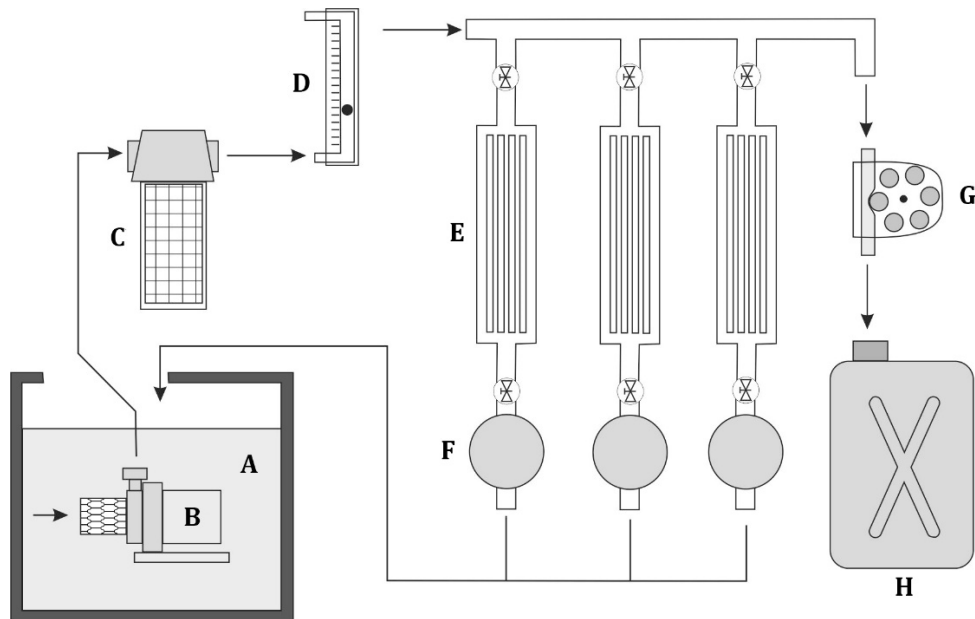
201 As the Grand-Chambéry sewer network does not fully separate storm waters from sewages, the study
202 was performed during a dry period to avoid any occasional high variations in mineral and organic
203 wastewater loads.

204

205 The specifically built automatic sampler (Figure 4) took water from the outlet of a trickling filters unit
206 during an adjustable pre-set time period (here 2.5 h and 5 h). Water temperature was about 15°C.
207 After flowing through a coarse meshed filter, the water was distributed across four channels, three of
208 them leading to probe chambers, each containing a PAC coated sampler-probe (PAC-S). PAC-S were
209 PAC-B similar 3D-printed structures, redesigned to fit the sampler chambers. The last channel led to a
210 peristaltic pump, set to take subsamples (volume adjusted to the experiment duration) every 5 min

211 during the 2.5 h or 5 h contact times. Collected subsamples were all poured into a 10 L container,
212 finally resulting in one single water sample integrated over the experiment period.

213



214

215 *Figure 4. Hydraulic circuit of the automatic sampler: A) trickling filters outlet collector tank, B) pump,*
216 *C) coarse filtration unit, D) rotameter, E) probe chambers, F) flow sensors, G) peristaltic pump, and H)*
217 *time-integrated water-collector.*

218 Channel flow rates were measured by flow sensors, and recorded, then used to standardise each
219 channel results for water discharge. At the end of the experiment, PAC-S and the time-integrated
220 water sample were recovered and conveyed at 4°C to the laboratory for virus analysis.

221

222 **2.8. Virus extraction from wastewater**

223 Virus were extracted from wastewater following a protocol derived from Pina *et al.* (1998). After the
224 wastewater sample was twice homogenized for 30 s at 13,000 rpm using a hand blender, 25 mL were
225 collected and spiked with MNV-1, to a $3.21 \cdot 10^7$ genome units.mL⁻¹ final concentration. The sample
226 was then mixed with 10 mL of 50 mM glycine and 3% beef extract buffer (pH 9.5) and incubated for
227 30 min at 4°C to promote the virus desorption from suspended matter. 10 mL of 2X phosphate buffer
228 saline (pH 7.2) were then added to the mixture for pH neutralisation, prior to be centrifugated (12,000
229 g for 15 min at 4°C). The pellet was discarded and the supernatant subjected to the nucleic acids'
230 extraction process.

231

232 **2.9. Nucleic acids extraction**

233 Nucleic acids extractions and purifications were carried out using NucliSENS® reagents (Biomérieux,
234 Marcy l'Étoile, France) and the semi-automatised eGENE-UP® platform (Biomérieux, Marcy l'Étoile,
235 France) according to slightly modified manufacturer instructions. Briefly, samples (either saline virus
236 suspensions from assays or wastewater from the automatic sampler experiments or the solid coated
237 devices: PAC-S, PAC-B and PAC-S) were mixed with 30 mL of lysis buffer for 30 min at room
238 temperature. In experiments on fPAC-F, lysis buffer volume was 2 mL. 50 µL of magnetic silica beads
239 were then added to the lysate and allowed to bind nucleic acids for 15 min at room temperature under
240 shaking. Beads were washed successively with the three NucliSENS® extraction buffers and eluted in
241 100 µL of the third one. Eluted beads were vortexed then heated for 5 min at 65°C and stirred at 1600
242 rpm, allowing the release of nucleic acids. After a 30 sec centrifugation at 480 g, the supernatant
243 (hereafter referred as RNA extract) was separated from the beads, carefully transferred into sterile
244 microcentrifuge tubes and stored at -20°C prior to analysis.

245

246 **2.10. Molecular quantification by RT-qPCR**

247 RT-qPCR was carried out using the TaqMan Fast Virus One-Step Master Mix from Applied
248 Biosystems™ (Waltham, MA, USA) with a total 20µL reaction volume. The reaction mixture contains
249 5µl of template, 5µL of Master Mix and primers and probes as needed per specific assay (Table 1).
250 MNV-1 and NoV GI were quantified in multiplex reaction, while AdV was quantified in simplex one.

251

252 Table 1 : primers and probe's sequences for each analysed virus

Matrix	Primers and probes	Primer and probes sequences (5' → 3')	Final concentration (nM)
Virus			
suspension in	MNV-1-F5006	TGGAACAATGGATGCTGA	400
NaCl 0.1M	MNV-1-R5078	GCTGCGCCATCACTC	800
and	MNV-1-P5028	(Texas red) CCGCAGGAACGCTCAGCAGT (BHQ-2)	100
Wastewater			
	NoVGI-F5279	CCATGTTCCGYTGGATG	600
Wastewater	NoVGI-R5372	CCTTAGACGCCATCATCAT	600
	NoVGI-P5326	(FAM) GATCGCRATCTYCTGCCCGAATT (BHQ-1)	300
	AdV_ABDEFG_F17676	TACATGCAYATCGCCG	300
Wastewater	AdV_ABDEFG_R17727	CGGGCRAAYTGCACC	900
	AdV_ABDEFG_P17694	(FAM) CAGGAYGCYTCGGARTAYCT (BHQ-1)	400

253

254 RT-qPCR was performed using a LightCycler 480 thermocycler (Roche, Basel, Switzerland), with the
 255 following thermal cycling conditions: 5 min at 50 °C, 5 min at 95 °C, and 45 cycles of 20 s at 95 °C
 256 followed by 40 s at 60 °C. Data were collected at the end of each cycle. Results were validated after
 257 corresponding viruses' positive control and autoclaved ultrapure water negative control.

258

259 2.11. Raw data formatting

260 LightCycler® 480 software (Roche, Basel, Switzerland) was used to analyse all RT-qPCR tests. Data
 261 were collected and managed in Microsoft Excel (Microsoft Corp., Redmond, WA, USA). Cycle
 262 threshold (Ct) levels were manually set at the starting points of samples' internal positive control
 263 exponential phase.

264 All samples with a Ct larger than 40 or replicates with a $\Delta Ct > 1$ were considered negative and
 265 discarded.

266 Differences between initial and final (after contact with the sorbent) virus concentrations in 0.1 M NaCl
 267 suspensions, were used as proxy of virus adsorptions on PAC materials.

268 Results from replicates were all summarised as medians (unknown data population distributions) and
269 Median Absolute Deviations were computed accordingly.

270 The percentage of virus retrieved from the sorbent or which disappeared from the suspension at the
271 end of adsorption experiments, was calculated as follows:

272

$$273 \quad Q \text{ (MNV-1 recovery rate) (\%)} = \frac{Q_f \text{ (viral RNA genome copies recovered)}}{Q_0 \text{ (viral RNA genome copies seeded)}} \times 100$$

274

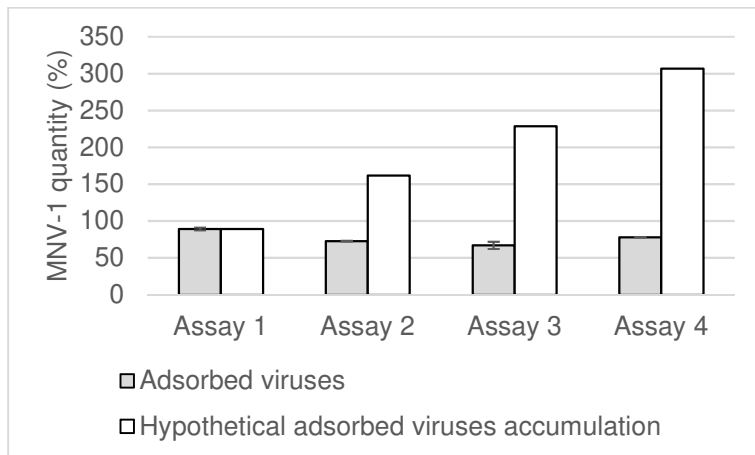
275

276 3. Results

277 3.1. Viruses' adsorption and desorption using PAC-coated devices

278 The experiment aimed at the measure of MNV-1 adsorption on PAC-F and at the analysis of its
279 repeatability.

280



281

282 *Figure 5. PAC-F 24h adsorption repeatability in 0.1M NaCl viral suspension. Error bars are ± Median*
283 *Absolute Deviation.*

284

285 As stated on *Figure 5*, adsorption in the first assay appeared significantly higher than in the three
286 following ones, attesting for a slight decrease of the sorbent adsorption capacity along the repeats. It
287 was asserting the progress of adsorption toward its saturation. However, this decrease did not amplify
288 from assay 2 to assay 4, despite each time virus accumulation on PAC-F was attested by the virus
289 concentration drop in the suspension.

290 After a first decrease, CNovel™ kept a significant adsorption capacity, even after a four-times
291 exposition to suspensions with same initial virus concentration. At the end of the experiment a total of
292 $8.69 \cdot 10^7$ viruses were then removed from the suspensions by the 0.038 ± 0.012 g PAC-F (*i.e.* $2.29 \cdot 10^9$
293 genome units.g⁻¹ of PAC).

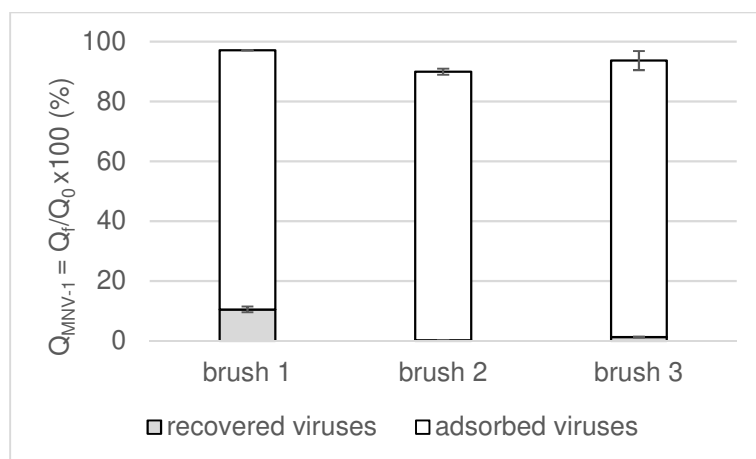
294

295 Virus adsorption was then investigated with PAC-B designed as field-operational probes candidates.

296 Compared to PAC-F, brushes coating resulted in a thin PAC layer, then with likely lower adsorption

297 capacity, but with larger active surface.

298



299

300 *Figure 6. PAC-B MNV-1 adsorption in 0.1M NaCl viral suspension and recovering efficacies. Error*
301 *bars are ± Median Absolute Deviation.*

302 MNV-1 adsorption on PAC-B 1, 2, and 3 (triplicates) reaches $97 \pm 0.03\%$, $90 \pm 1.03\%$ and $94 \pm 3.18\%$
303 respectively, after 24 h contact with the viral suspension (Figure 6). After desorption, $11 \pm 0.97\%$ of the
304 adsorbed viruses were recovered from the first brush, while $0.3 \pm 0.02\%$ and $1.4 \pm 0.14\%$, were
305 obtained from the second and third recovery assays, respectively.

306 Thus, despite their thin PAC layer, PAC-B demonstrated to be efficient adsorbent devices, with a final
307 adsorption of $2.63 \cdot 10^7$ viruses on the 1.2 ± 0.3 g of PAC-B (*i.e.* $2.19 \cdot 10^7$ genome units.g⁻¹ of PAC-B).

308 However, the desorption technique appeared rather inefficient on PAC-B, resulting in quite poor virus
309 retrieval values.

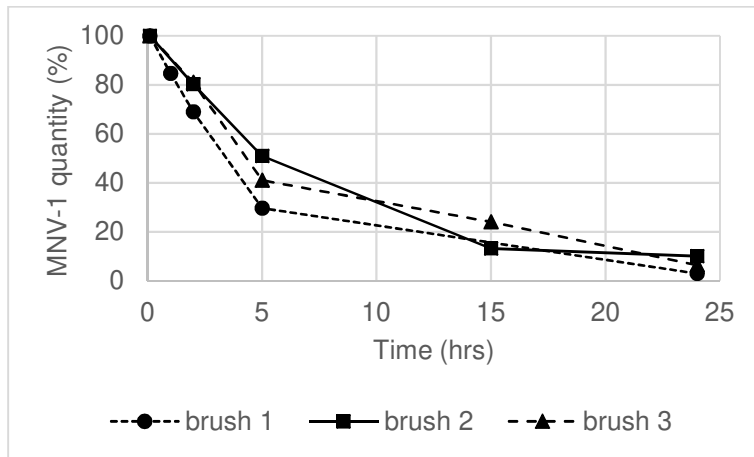
310

311 **3.2. Adsorption kinetics**

312 Short sampling time is a key parameter in field-operational tools performances. PAC-B adsorption
313 kinetics was therefore a focal point to be investigated.

314

315



316

317 *Figure 7. PAC-B adsorption kinetics in a 0.1M NaCl MNV-1 suspension. Values were calculated*
318 *according to the following formula: ratio (%) = concentration of remaining viruses at x h/initial virus*
319 *concentration x 100.*

320 Three successive assays delivered the similar adsorption kinetic patterns (Figure 7). Virus
321 concentration ranges from 30% to 51% after a 5h contact time, dropping to values as low as 10 to 3%
322 after 24h, when a nearly total adsorption of the initial virus load was observed.

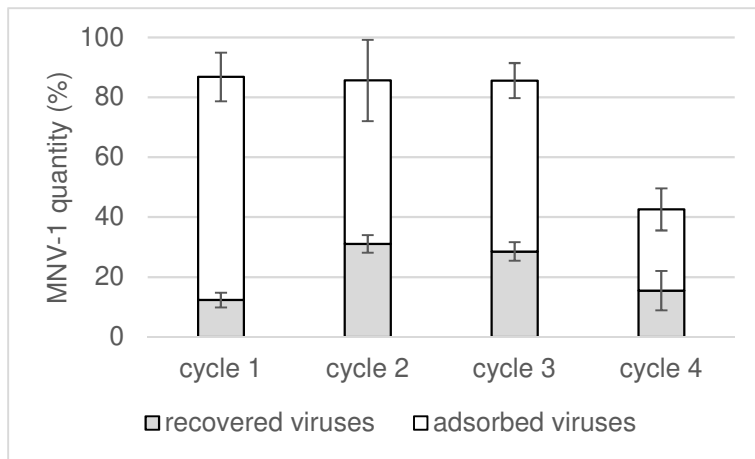
323

324 3.3. PAC reusability

325 PAC-F and PAC-B ability to be reused were studied with the perspective to use them in a field-
326 operational tool.

327 Reusability was investigated from steadiness performances of both the two steps of virus "adsorption"
328 sampling (alias virus concentration decrease in the 0.1 M NaCl suspension) and "recovery" (direct
329 retrieval of virus nucleic acids after submitting PAC to the lysis buffer).

330



331

332 *Figure 8. PAC-F reusability in the 0.1 M NaCl suspension assayed over four MNV-1*

333 *adsorption/recovery cycles. Error bars are ± Median Absolute Deviation.*

334 PAC-F reusability was tested over four virus adsorption/desorption cycles (Figure 8).

335 Adsorption efficiency kept quite steady during the firsts three cycles (85 to 86%), before falling to 43

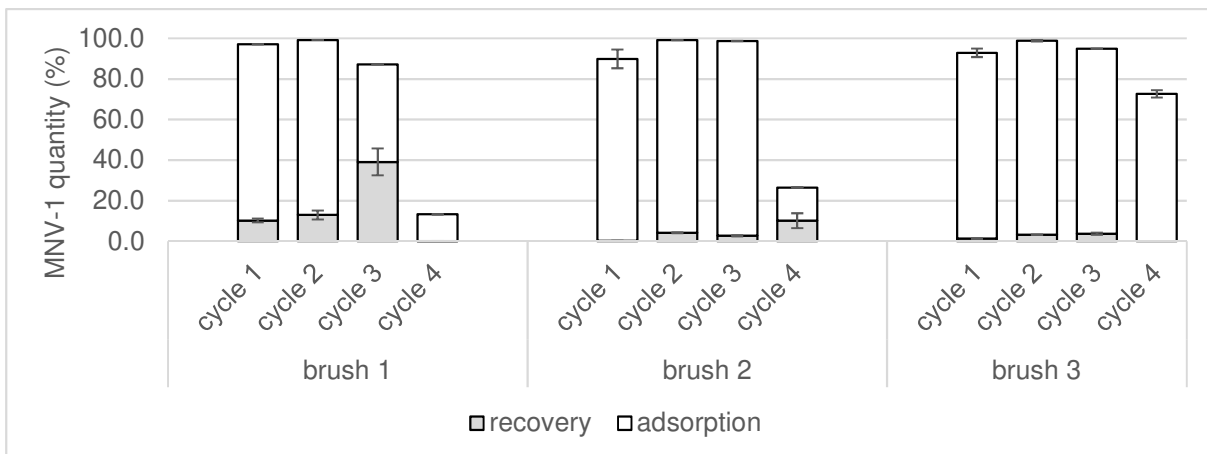
336 ±7% at the last one. Recovery rate was about 14 ±2% at the first cycle, and reached 36 ±3%, 33 ±3%

337 and 36 ±7% at cycles 2, 3 and 4, respectively.

338 One of the main outcomes of the experiment is the lowest adsorption uptake occurring at the last

339 assay. Despite the good performance of the recovery, with regard to this value, the result suggests

340 that three successive uses (adsorption + recovery) of PAC-F, only are possible.



341

342 *Figure 9. PAC coated brush (PAC-B) reusability during four adsorption/desorption cycles. Error*

343 *bars are ± Median Absolute Deviation.*

344 Four repeats of virus adsorption/desorption cycle were performed, to investigate the PAC-B

345 reusability. MNV-1 adsorption uptake rate ranged from 87 to 99 % during the first three cycles (Figure

346 9), then decreased to $13 \pm 0.00\%$, $16 \pm 0.02\%$ and $73 \pm 1.76\%$ with brushes 1, 2 and 3 respectively, at
347 the fourth cycle.

348 The corresponding virus recovery appeared slightly higher lately, after one or two reuses, especially
349 with brush 1 at the 3rd cycle. Results, from brushes 1 and 2, mainly, also suggest that differences in
350 PAC-coating masses, 1.56, 1.08 and 1.02 g on brushes 1, 2 and 3 respectively, were playing a part in
351 these recovery rate values.

352 These assays corroborated conclusions from foils experiments in that, under our experimental
353 conditions, PAC-devices (PAC-F and PAC-B) could hardly sustain more than three times reuses.

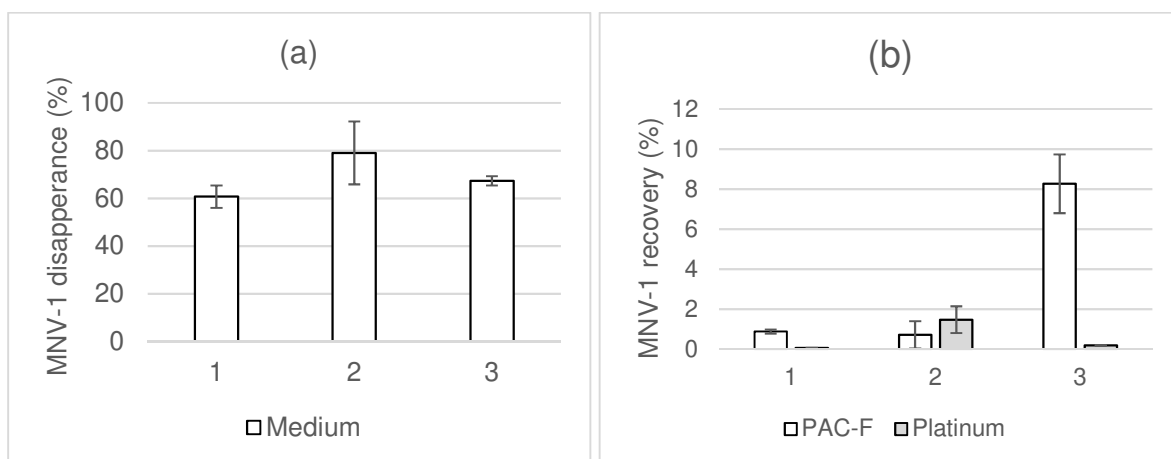
354

355 3.4. Polarization effect on PAC-F adsorption efficiency

356 Virus electrical charges play a major role in adsorption processes (Gerba, 1984). While large
357 variations according to species and groups, have been recorded, virus IP frequently establishes
358 between 3.5 and 7 (5.5 to 6.0 for Norwalk virus (Michen and Graule, 2010)). In environmental
359 freshwaters at pH between 6.5 and 7.5, and certainly in our 0.1M NaCl virus suspension, virus behave
360 as anions, justifying that one of the most usual sampling techniques rely on positively charged filtration
361 cartridges.

362 PAC-F polarisation experiments were designed to investigate a possible involvement of polarity in
363 CNovel™ MNV-1 adsorption efficacy.

364



365

366 *Figure 10. (a): Remaining virus in the 0.1 M NaCl MNV-1 suspension : at the end of the PAC-F*
367 *polarisation experiment. (b): MNV-1 recovery rates from PAC-F and platinum electrodes. 1. PAC-F as*
368 *anode. 2. PAC-F as cathode. 3. Unpolarised PAC-F. Error bars are \pm Median Absolute Deviation.*

369

370 Three experiments were planned, respectively with PAC-F as anode (1), PAC-F as cathode (2) and
371 with no polarisation (3), all with platinum foil as counter electrode.

372 As depicted on Figure 10 (a), PAC-F adsorption rate exhibited no clear significant difference whatever
373 its electrode status, suggesting that, under our experimental conditions the foil polarity didn't play a
374 meaningful part into virus adsorption efficacy. Here, the enforced polarisation probably did not shift the
375 equilibrium of adsorption.

376 This conclusion was corroborated by results on recovery rates (Figure 10 (b)) where highest values
377 appeared associated to non-polarised PAC-F assay (8%).

378 Such results were somewhat unexpected and could have been contrasted after adjustment of several
379 parameters. Among them, foils composition (percentages of PAC, PTFE and conductive carbon) and
380 varied applied voltages, within a narrow range, though, as the 0.9 V used during our experiments was
381 considered the highest safe possible potential before triggering water electrolysis.

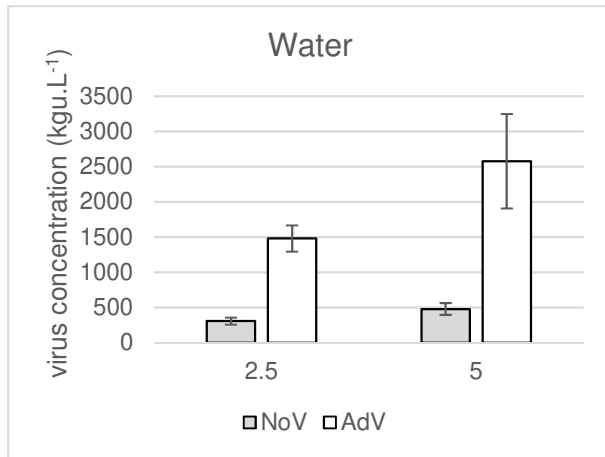
382

383 **3.5. Preliminary assays operating PAC-probes to sample wastewater autochthonous HEV**

384 Two types of samples were collected by the automatic sampler: PAC-S probes and a water sample
385 integrated over the experiment period (section 2.7).

386 Whereas virus concentrations could easily be calculated from water analyses, virus quantities only can
387 be derived from probes analyses, preventing all direct comparison of virus loads between water and
388 probes: PAC-probes should be seen as devices devoted to virus-detection, with no possible
389 standardisation by reference to the water volume that was flowing around.

390



391

392 *Figure 11. Concentrations of autochthonous NoV GI and AdV in the 2.5 h and 5 h integrated water.*

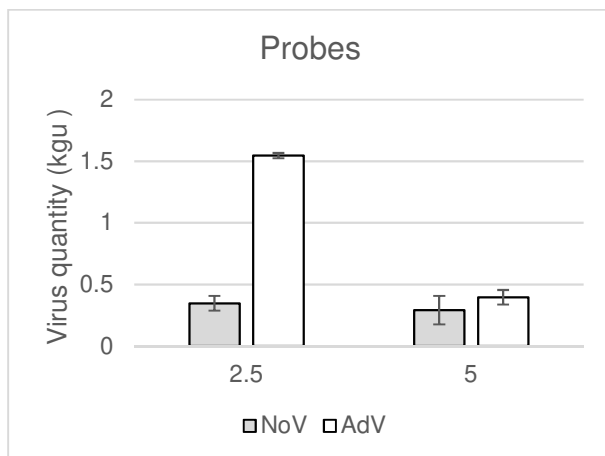
393 *Error bars are ± Median Absolute Deviation.*

394 Figure 11 exhibits the overall increase in HEV loads between the two investigated contact time periods
 395 (2.5 h and 5 h). This was certainly linked to water-related human activities, as the 5 h period
 396 encompassed the after-lunch water uses. For some reasons, the increase was slightly higher for AdV
 397 (72%) than for NoV GI (56%).

398 A similar pattern was given by the probes analysis (Figure 12) but only for the 2.5 h exposure time as
 399 both virus groups found in water were also detected with PAC-Sand at the same ratio (Figure 12).

400

401



402

403 *Figure 12. Amount of autochthonous NoV GI and AdV recovered from the PAC-S after 2.5 h and 5*
 404 *h contact time with wastewater. Error bars are ± Median Absolute Deviation.*

405 A sharp decrease in the retrieved AdV load was observed after 5 h contact time, while twice the water
 406 volume of the 2.5 h period flowed through the probes (a total of 323 L). Probes clogging processes

407 were likely to explain this result, as exemplified by a previous 24 h exposition-period experiment when
408 no virus were detected due to a conspicuous clogging making totally inefficient the virus extraction
409 technique (data not shown).

410 NoV GI appeared to be less affected than AdV by these hindrances, probably as a result of their
411 differences in capsid size and peripheral structures: two decisive parameters for their diffusion speed
412 (Zhdanov and Kasemo, 2010) and for the strength of their interactions with the activated carbon
413 surface. The larger AdV capsid (about 80 nm in diameter) would thus be less likely adsorbed on
414 clogged PAC-S than the smaller NoV GI (about 30 nm in diameter) (Kapikian *et al.*, 1972).

415

416 **4. Discussion**

417

418 Our work intended to shape and validate PAC-based virus sampling tools, allowing their recovery for
419 further analysis in a whole catch 'n' retrieve two steps procedure. First, it should be pointed out that
420 most experiments were performed using MNV-1 suspensions. Even though it is an accepted surrogate
421 of human noroviruses, our results cannot be extended to other viruses without further experiments,
422 especially regarding the capsid size and properties such as the isoelectric point.

423

424 Implemented into our PAC-devices (foils and brushes), CNovel™ powdered activated carbon proved
425 to be a very efficient MNV-1 adsorbent, demonstrating no saturation within the scope of our
426 experiments. Our values of its adsorption efficacy cannot be easily compared to similar studies
427 dedicated to virus adsorption on activated carbon, as most of them, dealt with virus integrity
428 (/infectivity) therefore reporting adsorption efficacies as PFU.L⁻¹ (Matsushita *et al.*, 2013; Domagala *et*
429 *al.*, 2021; Shimabuku *et al.*, 2018). A comparison may yet be tempted with some results from Cormier
430 *et al.* (2014) putting forward a ratio of 9.18 genome units per PFU. After conversion, their PFU results
431 indicated that 9.10^6 to 6.10^7 MS2 genome units were adsorbed on 1 g of GAC in 2 h 45', whereas it
432 took 24 h for 1g CNovel™ to adsorbed $2.19.10^7$ MNV1 genome units. The two viruses, MS2 and MNV-
433 1 being similar in size, the comparison is suggesting that GAC adsorption kinetics would be faster than
434 CNovel™ foil one (PAC-F). However, the difference could also be related to the high contribution of
435 salinity in virus adsorption efficacy supported by Cormier *et al* (2014). According to their results, at
436 20°C, the optimal salinity was about at 20 ppt, whereas salinity in our 0.1M NaCl MNV-1 suspension

437 was only 5.8 ppt. This comparison emphasized the fact that the adsorption capacities of PAC included
438 in probes designed for virus sampling in wastewaters or other freshwaters, should be high enough to
439 compensate for working far from their optimum conditions.

440

441 Polarisation of PAC foils appeared to be no help in virus adsorption improvement under our
442 experimental conditions. The results suggested that virus polarity at pH 7 (conditions chosen close to
443 the ones in sewage treatment plants) was not enough oriented toward an anionic or cationic behaviour
444 which would trigger effective adsorption enhancement. They advocate for further experiments where
445 polarity would be applied over short periods and with some adjustments of foils' composition.

446

447 CNovel™ appeared to be able to withstand some reusability, keeping a high and fairly constant
448 adsorption efficacy over 3 repeats similarly with both, PAC-F and PAC-B (*Figure 8* and *Figure 9*), then
449 suggesting the involvement of device-independent parameters in this limitation that will be reviewed
450 later in this discussion.

451 Bad between-brushes reproducibility (*Figure 9*) highlighted the difficulty to produce exact copies of
452 hand-craft PAC-based devices. PAC coating was difficult to reproduce, leading to between-brushes
453 differences in amount, thickness and evenness of the activated carbon layer. Making use of an
454 automatic coating machine would be a better choice in future experiments. This is why, results from
455 brush 1, the one with the highest PAC weight, mainly, will be considered in the following discussions.

456

457 Adsorption kinetic on PAC-B followed a slow exponential decay (*Figure 7*). A similar figure was
458 described by Cormier *et al.* (2014) in their experiments where GAC was added to seawater spiked with
459 MS2 bacteriophages.

460 Such pattern may be derived from a simple diffusion-controlled adsorption which apply to all particle
461 suspensions in contact with an adsorbent under constant temperature and zero velocity (Zhdanov and
462 Kasemo, 2010). Temperature was constant in our experiments (20°C), however, a reciprocal shaker
463 allowed some sort of stirring of both, brushes and virus suspension, then increasing the probability
464 viruses came into contact with the activated carbon. As virus concentration decreased due to the
465 adsorption, the concentration gradient between viruses and activated carbon was decreasing and
466 consequently the diffusion flow speed decreased as well as the adsorption rate. Actually, the figure

467 was probably more complex: when working with non-planar activated carbon surfaces, particles
468 transport limitation comes not only from diffusion but also from some shapes' parameters of the
469 activated carbon, like particles radius in the case of activated carbon powder (Alvarez *et al.*, 2010).
470 Adsorption rate decrease could also be explained by a self-limiting process where adsorption impaired
471 itself because of the progressive saturation of the adsorption sites by the adsorbed virus. In addition,
472 the lysis buffer action at the end of each adsorption/ recovery cycle, probably left debris and molecules
473 (proteins) which were not all collected with the buffer and in a number much higher than the initial
474 number of intact viruses. Both, processes, diffusion-controlled adsorption and adsorption drift to
475 saturation, were likely main contributors in the adsorption rate decrease (Figure 7) and the one
476 observed at cycle 4 for PAC devices reusability experiments, occurring with both, PAC-F and PAC-B
477 (Figure 8 and Figure 9).

478
479 Unlike adsorption, virus recovery measurements yielded contrasted, quite low and highly variable
480 values in all our experiments. A maximum of 40% virus recovery was registered from one of our
481 brushes after 3 times reuse and a few percent only, from the two other brushes, during the same
482 experiment. Aside their volatility, these results represented a significant progress where other authors
483 just failed to isolate RNA from powdered activated carbon (Cormier *et al.*, 2014). However, they still
484 are questioning the processes from which they derived, probably related to conflicting parameters,
485 some impairing, some promoting the underlying reactions.

486
487 The performance of the adsorbed virus recovery process was primarily explained by the one of the
488 NucliSENS® lysis buffer. It was relying from both its composition and its ability to reach and react with
489 the virus while its diffusion progressed into the PAC porosity and the bulk of mineral and organic
490 material that might be deposited on it. Results from our reusability experiments, both with foils (PAC-F)
491 and brushes (PAC-B) illustrated the way this material covering the activated carbon might have
492 interfered with the operability of the buffer. Lowest values of recovery rate always occurred at the 1st
493 use of either PAC-F or PAC-B (Figure 8 and Figure 9, brush 1). At this time, a bare PAC surface was
494 exposed to the virus suspension. It can be expected that the strength of adsorption forces (van der
495 Walls and electrostatic) were then at their maximum. Two reasons might explain a poor performance
496 of the buffer, at the moment:

497 - 1) RNAs released from the virus lysis, might have been adsorbed by the activated carbon and then
498 no longer able to be collected by the buffer. Such an adsorption was demonstrated with DNAs and
499 RNAs solutions on materials like graphene, nanotubes or biochar (Kirtane *et al.*, 2015; Pividori and
500 Alegret, 2005; Bimová *et al.*, 2021). Conversely, other studies were suggesting that PAC may improve
501 DNA analysis by removing some qPCR inhibitors like humic acids (Barbaric *et al.*, 2015), a benefit
502 which was not evidenced in our measures.

503 - 2) Part of the buffer could be made ineffective by its contact with the activated carbon after its
504 components were dissociated, due to differences in their affinities with the carbon adsorption sites.
505 Indeed, both thiocyanate and EDTA could be adsorbed on activated carbon with different efficacies as
506 reported by Aguirre *et al.* (2010) and Zhu *et al.* (2011) on activated carbons with similar BET surface
507 areas.

508

509 *Figure 8* and *Figure 9* also show that the virus recovery rate increased at cycles 2 and 3, with both,
510 foils and brushes. At this time, part of the PAC porosity might be clogged by virus debris (capsid
511 and/or protein residuals) and some virus left untouched by the lysis buffer, from the previous assay.
512 We may assume that the consequences of this extra layer were to maintain newly released RNA a bit
513 farther from the active carbon, then lowering the adsorption forces and consequently easing its
514 collection by the lysis buffer. This interpretation is consistent with the expected decrease of adsorbate
515 interaction energy when adsorption uptake increases, as observed by Baker *et al.* (2010) with
516 heterogeneous surfaces, such as our PAC coating.

517

518 Briefly, four processes were probably contributing to these low values of virus recovery: 1. of course
519 the adsorption itself with the amount of virus collected, 2. lysis buffer inability to reach adsorbed virus
520 3. its dissociation, and 4. RNA adsorption. All are related to the amount of proteins and debris clogging
521 the activated carbon which should be large enough for weakening adsorption forces. However, they
522 shouldn't be too overwhelming, then shielding the carbon surface from new contacts with viruses, and
523 obstructing lysis buffer reaching already adsorbed viruses.

524

525 Optimal conditions for an efficient "catch 'n' retrieve" virus sampling protocol, probably laid within a
526 narrow range of activated carbon obstruction, as demonstrated when adsorption itself came to be

527 affected. It occurred at cycle 4 of our reusability experiments, whatever the PAC device (foils or
528 brushes). At this time, a value of virus recovery could be registered from brush 2 but not from brush 1,
529 while, in both cases, virus adsorption was low (*Figure 9*). According to our assays and the way our
530 PAC devices were designed, such a trade-off appeared to be met after two to three reuses of the
531 devices.

532

533 Field experiments involving our PAC-S, demonstrated that adsorbent based probes were able to
534 endure wastewater harsh conditions, for short exposition periods, allowing the retrieval of part of the
535 HEV autochthonous load and part of its diversity (*Figure 12*). Significant amount of virus was collected
536 despite a quite low temperature (15°C). This result appeared to be in line with studies supporting for
537 no temperature effect on protein adsorption on activated carbon, at least within the range of
538 wastewater's temperatures (Cookson, 1969). The exposition period should be optimized to
539 compromise for the aforementioned trade-off between beneficial clogging and lysis buffer efficacy, a
540 threshold that was obviously outreached with the 5 h exposition time.

541

542 **5. Conclusion**

543 One of the main achievements of this work was to set up and validate PAC-based devices. Supported
544 by a performing adsorption and despite some volatility of the recovery step, our catch 'n' retrieve
545 protocol, in association with our CNovel™-based sampling tools (PAC-B and PAC-S particularly) were
546 able to supply virus samples to downstream molecular analysis. Our experiments highlighted the
547 importance of two parameters in operating PAC-based devices: 1) the choice of an exposition time
548 balancing efficient adsorption and virus recovery 2) the need for a pre-use probes conditioning (pre-
549 use allowing some degree of clogging of the activated carbon porosity) which compensate in part, for
550 the too effective adsorption forces of the CNovel™.

551

552 **6. Acknowledgments**

553 The research was supported by the ABIOLAB laboratory (Montbonnot Saint-Martin, France), where
554 most experiments were performed and by the ASPOSAN association.

555 Fields experiments were possible thanks to the Grand Chambéry WWTP authorities. Their help in
556 setting up the automatic sampler at the trickling filters outlet was greatly appreciated.

557

558 7. References

559 Aguirre, N.V., Vivas, B.P., Montes-Morán, M.A., Ania, C.O., 2010. Adsorption of Thiocyanate Anions from
560 Aqueous Solution onto Adsorbents of Various Origin. *Adsorption Science & Technology* 28, 705–716.

561 <https://doi.org/10.1260/0263-6174.28.8-9.705>

562 Ahmed, W., Bertsch, P.M., Bivins, A., Bibby, K., Farkas, K., Gathercole, A., Haramoto, E., Gyawali, P.,

563 Korajkic, A., McMinn, B.R., Mueller, J.F., Simpson, S.L., Smith, W.J.M., Symonds, E.M., Thomas,

564 K.V., Verhagen, R., Kitajima, M., 2020. Comparison of virus concentration methods for the RT-qPCR-

565 based recovery of murine hepatitis virus, a surrogate for SARS-CoV-2 from untreated wastewater.

566 *Science of The Total Environment* 739, 139960. <https://doi.org/10.1016/j.scitotenv.2020.139960>

567 Albinana-Gimenez, N., Clemente-Casares, P., Calgua, B., Huguet, J.M., Courtois, S., Girones, R., 2009.

568 Comparison of methods for concentrating human adenoviruses, polyomavirus JC and noroviruses in

569 source waters and drinking water using quantitative PCR. *Journal of Virological Methods* 158, 104–

570 109. <https://doi.org/10.1016/j.jviromet.2009.02.004>

571 Alvarez, N.J., Walker, L.M., Anna, S.L., 2010. Diffusion-limited adsorption to a spherical geometry: The

572 impact of curvature and competitive time scales. *Phys. Rev. E* 82, 011604.

573 <https://doi.org/10.1103/PhysRevE.82.011604>

574 Aslan, A., Xagorarakis, I., Simmons, F.J., Rose, J.B., Dorevitch, S., 2011. Occurrence of adenovirus and

575 other enteric viruses in limited-contact freshwater recreational areas and bathing waters. *Journal of*

576 *Applied Microbiology*. <https://doi.org/10.1111/j.1365-2672.2011.05130.x>

577 Bae, J., Schwab, K.J., 2008. Evaluation of Murine Norovirus, Feline Calicivirus, Poliovirus, and MS2 as

578 Surrogates for Human Norovirus in a Model of Viral Persistence in Surface Water and Groundwater.

579 *Appl Environ Microbiol* 74, 477–484. <https://doi.org/10.1128/AEM.02095-06>

580 Baker, T.A., Kaxiras, E. & Friend, C.M. Insights from Theory on the Relationship Between Surface

581 Reactivity and Gold Atom Release. *Top Catal* 53, 365–377 (2010). <https://doi.org/10.1007/s11244->

582 010-9446-3

583 Barbarić, L., Bačić, I., Grubić, Z., 2015. Powdered Activated Carbon: An Alternative Approach to Genomic

584 DNA Purification. *J Forensic Sci* 60, 1012–1015. <https://doi.org/10.1111/1556-4029.12773>

585 Bimová, P., Roupcová, P., Klouda, K., Matějová, L., Staňová, A.V., Grabicová, K., Grabic, R., Majová, V.,
586 Híveš, J., Špalková, V., Gemeiner, P., Celec, P., Konečná, B., Bírošová, L., Krahulcová, M.,
587 Mackuľak, T., 2021. Biochar – An efficient sorption material for the removal of pharmaceutically active
588 compounds, DNA and RNA fragments from wastewater. *Journal of Environmental Chemical*
589 *Engineering* 9, 105746. <https://doi.org/10.1016/j.jece.2021.105746>

590 Blacklow, N.R., Greenberg, H.B., 1991. Viral Gastroenteritis. *N Engl J Med* 325, 252–264.
591 <https://doi.org/10.1056/NEJM199107253250406>

592 Bouseettine, R., Hassou, N., Bessi, H., Ennaji, M.M., 2020. Waterborne Transmission of Enteric Viruses
593 and Their Impact on Public Health, in: *Emerging and Reemerging Viral Pathogens*. Elsevier, pp. 907–
594 932. <https://doi.org/10.1016/B978-0-12-819400-3.00040-5>

595 Canh, V.D., Osawa, H., Inoue, K., Kasuga, I., Takizawa, S., Furumai, H., Katayama, H., 2019.
596 Ferrihydrite treatment to mitigate inhibition of RT-qPCR virus detection from large-volume
597 environmental water samples. *Journal of Virological Methods* 236, 60-67.
598 <https://doi.org/10.1016/j.jviromet.2018.10.018>

599 Cioffi, B., Monini, M., Salamone, M., Pellicanò, R., Di Bartolo, I., Guida, M., La Rosa, G., Fusco, G., 2020.
600 Environmental surveillance of human enteric viruses in wastewaters, groundwater, surface water and
601 sediments of Campania Region. *Regional Studies in Marine Science* 38, 101368.
602 <https://doi.org/10.1016/j.rsma.2020.101368>

603 Cookson, J.T., North, W.J., 1967. Adsorption of viruses on activated carbon. Equilibriums and kinetics of
604 the attachment of Escherichia coli bacteriophage T4 on activated carbon. *Environ. Sci. Technol.* 1, 46–
605 52. <https://doi.org/10.1021/es60001a002>

606 Cookson, J.T., 1969. MECHANISM OF VIRUS ADSORPTION ON ACTIVATED CARBON. *Journal -*
607 *American Water Works Association* 61, 52–56. <https://doi.org/10.1002/j.1551-8833.1969.tb03702.x>

608 Cormier, J., Gutierrez, M., Goodridge, L., Janes, M., 2014. Concentration of enteric virus indicator from
609 seawater using granular activated carbon. *Journal of Virological Methods* 196, 212–218.
610 <https://doi.org/10.1016/j.jviromet.2013.11.008>

611 Crini, G., Lichtfouse, E., Wilson, L.D., Morin-Crini, N., 2019. Conventional and non-conventional
612 adsorbents for wastewater treatment. *Environ Chem Lett* 17, 195–213. [https://doi.org/10.1007/s10311-](https://doi.org/10.1007/s10311-018-0786-8)
613 [018-0786-8](https://doi.org/10.1007/s10311-018-0786-8)

614 Domagała, K., Bell, J., Yüzbaşı, N.S., Sinnet, B., Kata, D., Graule, T., 2021. Virus removal from drinking
615 water using modified activated carbon fibers. *RSC Adv.* 11, 31547–31556.
616 <https://doi.org/10.1039/D1RA06373A>

617 Enserink, R., van den Wijngaard, C., Bruijning-Verhagen, P., van Asten, L., Mughini-Gras, L., Duizer, E.,
618 Kortbeek, T., Scholts, R., Nagelkerke, N., Smit, H.A., Kooistra-Smid, M., van Pelt, W., 2015.
619 Gastroenteritis Attributable to 16 Enteropathogens in Children Attending Day Care: Significant Effects
620 of Rotavirus, Norovirus, Astrovirus, Cryptosporidium and Giardia. *Pediatric Infectious Disease Journal*
621 34, 5–10. <https://doi.org/10.1097/INF.0000000000000472>

622 Gerba, C.P., Sobsey, M.D., Wallis, C., Meinick, J.L., 1975. Adsorption of poliovirus onto activated carbon
623 in waste water. *Environ. Sci. Technol.* 9, 727–731. <https://doi.org/10.1021/es60106a009>

624 Gerba, C.P., 1984. Applied and Theoretical Aspects of Virus Adsorption to Surfaces, in: *Advances in*
625 *Applied Microbiology*. Elsevier, pp. 133–168. [https://doi.org/10.1016/S0065-2164\(08\)70054-6](https://doi.org/10.1016/S0065-2164(08)70054-6)

626 Gerba, C.P., 2000. Assessment of Enteric Pathogen Shedding by Bathers during Recreational Activity
627 and its Impact on Water Quality. *Quantitative Microbiology*, 2(1), 55-68.
628 <https://doi.org/10.1023/A:1010000230103>

629 Goldin, M.M., Volkov, A.G., Namyshkin, D.N., Filatova, E.A., Revina, A.A., 2005. Adsorption of Copper
630 and Calcium Cations on Polarized Activated Carbon Modified by Quercetin. *J. Electrochem. Soc.* 152,
631 E172. <https://doi.org/10.1149/1.1882032>

632 Hjelmsø, M.H., Hellmér, M., Fernandez-Cassi, X., Timoneda, N., Lukjancenka, O., Seidel, M., Elsässer,
633 D., Aarestrup, F.M., Löfström, C., Bofill-Mas, S., Abril, J.F., Girones, R., Schultz, A.C., 2017.
634 Evaluation of Methods for the Concentration and Extraction of Viruses from Sewage in the Context of
635 Metagenomic Sequencing. *PLoS ONE* 12, e0170199. <https://doi.org/10.1371/journal.pone.0170199>

636 Hmaïed, F., Jebri, S., Saavedra, M.E.R., Yahya, M., Amri, I., Lucena, F., Hamdi, M., 2016. Comparison of
637 Two Concentration Methods for the Molecular Detection of Enteroviruses in Raw and Treated
638 Sewage. *Curr Microbiol* 72, 12–18. <https://doi.org/10.1007/s00284-015-0909-4>

639 Janahi, E.M., Mustafa, S., Parkar, S.F.D., Naser, H.A., Eisa, Z.M., 2020. Detection of Enteric Viruses and
640 Bacterial Indicators in a Sewage Treatment Center and Shallow Water Bay. *IJERPH* 17, 6483.
641 <https://doi.org/10.3390/ijerph17186483>

642 Kapikian, A.Z., Wyatt, R.G., Dolin, R., Thornhill, T.S., Kalica, A.R., Chanock, R.M., 1972. Visualization by
643 Immune Electron Microscopy of a 27-nm Particle Associated with Acute Infectious Nonbacterial
644 Gastroenteritis. *J Virol* 10, 1075–1081. <https://doi.org/10.1128/jvi.10.5.1075-1081.1972>

645 Kauppinen, A., Pitkänen, T., Miettinen, I.T., 2018. Persistent Norovirus Contamination of Groundwater
646 Supplies in Two Waterborne Outbreaks. *Food Environ Virol* 10, 39–50. [https://doi.org/10.1007/s12560-](https://doi.org/10.1007/s12560-017-9320-6)
647 017-9320-6

648 Kirtane, A., Atkinson, J.D., Sassoubre, L., 2020. Design and Validation of Passive Environmental DNA
649 Samplers Using Granular Activated Carbon and Montmorillonite Clay. *Environ. Sci. Technol.* 54,
650 11961–11970. <https://doi.org/10.1021/acs.est.0c01863>

651 Martín-Díaz, J., Lucena, F., 2018. Extraction and RT-qPCR detection of enteroviruses from solid
652 environmental matrixes: Method decision tree for different sample types and viral concentrations.
653 *Journal of Virological Methods* 251, 145–150. <https://doi.org/10.1016/j.jviromet.2017.10.004>

654 Masclaux, F.G., Hotz, P., Friedli, D., Savova-Bianchi, D., Oppliger, A., 2013. High occurrence of hepatitis
655 E virus in samples from wastewater treatment plants in Switzerland and comparison with other enteric
656 viruses. *Water Research* 47, 5101–5109. <https://doi.org/10.1016/j.watres.2013.05.050>

657 Matsushita, T., Suzuki, H., Shirasaki, N., Matsui, Y., Ohno, K., 2013. Adsorptive virus removal with super-
658 powdered activated carbon. *Separation and Purification Technology* 107, 79–84.
659 <https://doi.org/10.1016/j.seppur.2013.01.017>

660 Michen, B., Graule, T., 2010. Isoelectric points of viruses. *Journal of Applied Microbiology* 109, 388–397.
661 <https://doi.org/10.1111/j.1365-2672.2010.04663.x>

662 Pina, S., Jofre, J., Emerson, S.U., Purcell, R.H., Girones, R., 1998. Characterization of a Strain of
663 Infectious Hepatitis E Virus Isolated from Sewage in an Area where Hepatitis E Is Not Endemic. *Appl.*
664 *Environ. Microbiol.* 4. <https://doi.org/10.1128/AEM.64.11.4485-4488.1998>

665 Pividori, M.I., Alegret, S., 2005. DNA Adsorption on Carbonaceous Materials, in: Wittmann, C. (Ed.),
666 Immobilisation of DNA on Chips I, Topics in Current Chemistry. Springer-Verlag, Berlin/Heidelberg, pp.
667 1–36. <https://doi.org/10.1007/b136064>

668 Powell, T., Brion, G.M., Jagtoyen, M., Derbyshire, F., 2000. Investigating the Effect of Carbon Shape on
669 Virus Adsorption. *Environ. Sci. Technol.* 34, 2779–2783. <https://doi.org/10.1021/es991097w>

670 Prado, T., de Castro Bruni, A., Barbosa, M.R.F., Garcia, S.C., de Jesus Melo, A.M., Sato, M.I.Z., 2019.
671 Performance of wastewater reclamation systems in enteric virus removal. *Science of The Total*
672 *Environment* 678, 33–42. <https://doi.org/10.1016/j.scitotenv.2019.04.435>

673 Prata, C., Ribeiro, A., Cunha, Â., Gomes, Newton.C.M., Almeida, A., 2012. Ultracentrifugation as a direct
674 method to concentrate viruses in environmental waters: virus-like particle enumeration as a new
675 approach to determine the efficiency of recovery. *J. Environ. Monit.* 14, 64–70.
676 <https://doi.org/10.1039/C1EM10603A>

677 Qiu, Y., Lee, B.E., Neumann, N., Ashbolt, N., Craik, S., Maal-Bared, R., Pang, X.L., 2015. Assessment of
678 human virus removal during municipal wastewater treatment in Edmonton, Canada. *J Appl Microbiol*
679 119, 1729–1739. <https://doi.org/10.1111/jam.12971>

680 Robles, I., Moreno-Rubio, G., García-Espinoza, J.D., Martínez-Sánchez, C., Rodríguez, A., Meas-Vong,
681 Y., Rodríguez-Valadez, F.J., Godínez, L.A., 2020. Study of polarized activated carbon filters as
682 simultaneous adsorbent and 3D-type electrode materials for electro-Fenton reactors. *Journal of*
683 *Environmental Chemical Engineering* 8, 104414. <https://doi.org/10.1016/j.jece.2020.104414>

684 Seitz, S.R., Leon, J.S., Schwab, K.J., Lyon, G.M., Dowd, M., McDaniels, M., Abdulhafid, G., Fernandez,
685 M.L., Lindesmith, L.C., Baric, R.S., Moe, C.L., 2011. Norovirus Infectivity in Humans and Persistence
686 in Water. *Appl. Environ. Microbiol.* 77, 6884–6888. <https://doi.org/10.1128/AEM.05806-11>

687 Sharkey, M.E., Kumar, N., Mantero, A.M.A., Babler, K.M., Boone, M.M., Cardentey, Y., Cortizas, E.M.,
688 Grills, G.S., Herrin, J., Kemper, J.M., Kenney, R., Kobetz, E., Laine, J., Lamar, W.E., Mader, C.C.,
689 Mason, C.E., Quintero, A.Z., Reding, B.D., Roca, M.A., Ryon, K., Solle, N.S., Schürer, S.C., Shukla,
690 B., Stevenson, M., Stone, T., Tallon, J.J., Venkatapuram, S.S., Vidovic, D., Williams, S.L., Young, B.,
691 Solo-Gabriele, H.M., 2021. Lessons learned from SARS-CoV-2 measurements in wastewater. *Science*
692 *of The Total Environment* 798, 149177. <https://doi.org/10.1016/j.scitotenv.2021.149177>

693 Shimabuku, Q.L., Ueda-Nakamura, T., Bergamasco, R., Fagundes-Klen, M.R., 2018. Chick-Watson
694 kinetics of virus inactivation with granular activated carbon modified with silver nanoparticles and/or
695 copper oxide. *Process Safety and Environmental Protection* 117, 33–42.
696 <https://doi.org/10.1016/j.psep.2018.04.005>

697 Sidhu, J.P.S., Sena, K., Hodggers, L., Palmer, A., Toze, S., 2018. Comparative enteric viruses and
698 coliphage removal during wastewater treatment processes in a sub-tropical environment. *Science of*
699 *The Total Environment* 616–617, 669–677. <https://doi.org/10.1016/j.scitotenv.2017.10.265>

700 Sinclair, R.G., Jones, E.L., Gerba, C.P., 2009. Viruses in recreational water-borne disease outbreaks a
701 review. *Journal of Applied Microbiology*. <https://doi.org/10.1111/j.1365-2672.2009.04367.x>

702 Soto-Beltran, M., Ikner, L.A., Bright, K.R., 2013. Effectiveness of Poliovirus Concentration and Recovery
703 from Treated Wastewater by Two Electropositive Filter Methods. *Food Environ Virol* 5, 91–96.
704 <https://doi.org/10.1007/s12560-013-9104-6>

705 Strubbia, S., Schaeffer, J., Oude Munnink, B.B., Besnard, A., Phan, M.V.T., Nieuwenhuijse, D.F., de
706 Graaf, M., Schapendonk, C.M.E., Wacrenier, C., Cotten, M., Koopmans, M.P.G., Le Guyader, F.S.,
707 2019. Metavirome Sequencing to Evaluate Norovirus Diversity in Sewage and Related
708 Bioaccumulated Oysters. *Front. Microbiol.* 10, 2394. <https://doi.org/10.3389/fmicb.2019.02394>

709 Zhdanov, V.P., Kasemo, B., 2010. Diffusion-limited kinetics of adsorption of biomolecules on supported
710 nanoparticles. *Colloids and Surfaces B: Biointerfaces* 76, 28–31.
711 <https://doi.org/10.1016/j.colsurfb.2009.10.004>

712 Zhu, H., Yang, X., Mao, Y., Chen, Y., Long, X., Yuan, W., 2011. Adsorption of EDTA on activated carbon
713 from aqueous solutions. *Journal of Hazardous Materials* 185, 951–957.
714 <https://doi.org/10.1016/j.jhazmat.2010.09.112>